Compact Stars

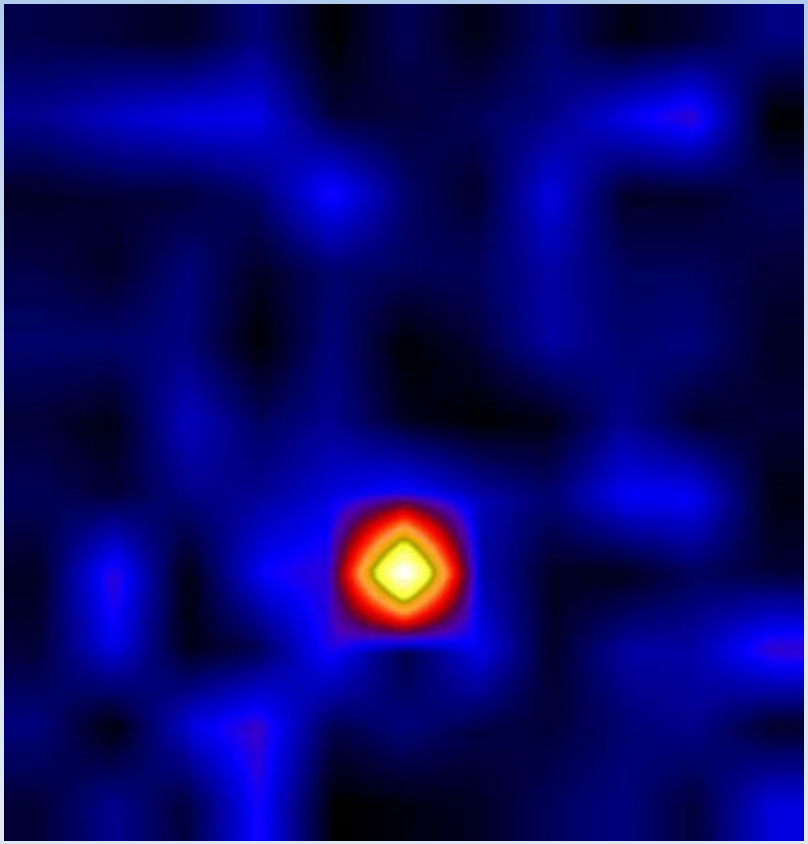

Lecture 10

Summary of previous lecture

- I presented the GRB central engine models, to explain how the relativistic jets are launched in short and long GRBs.
- The GRB engine accretion disks are dense and hot, so electron gas is degenerate. Its pressure does not depend on temperature, and scales with density with 5/3 or 4/3 power-law.
- These engines are opaque to photons, but neutrino cooling, and/or advection, can balance the viscous heating

Summary of previous lecture

- Accretion disks in GRB engines can be partially opaque to neutrinos, where these species are trapped and absorbed. Neutrino pressure also adds contribution to total pressure.
- Instabilities in the disk: thermal or gravitational, can lead to variable central engine activity. May be stabilized by torque transferred from rotating black hole.
- Nucleosynthesis of heavy elements up to Nickel possible via NSE in the outskirst of the disk.
- Rapid neutron capture in the outflows leads to formation of much heavier nuclei, up to Uranium and Thor. (Confirmed by discovery of a kilonova.)

Today: Neutron Stars

- Today I will talk about Neutron Stars.
- Single NS, their internal structure models, their maximal mass, and mass-radius relation, were studied since 1930’s
- I will discuss various equations of state (EOS).
- The BNS mergers, and in systems with NS-BH pairs, are progenitors of short gamma ray bursts and emit gravitational waves.
- Further constraints for the neutron star EOS can be given by merger observations

Neutron star history

- Discovery of neutron: 1932, J. Chadwick
- 1931: Landau and Bohr considered stars where nuclei are separated by size of a proton, $l \sim 10^{-13}$ cm
- The corresponding size of a star of 1 Solar mass will be $R \sim 12$ km

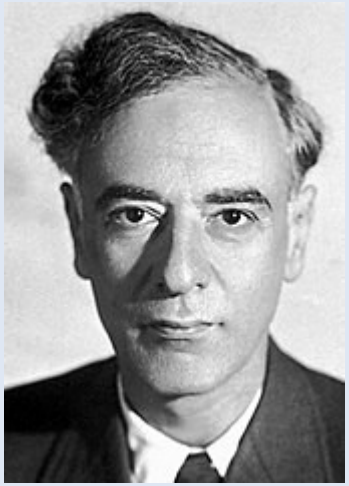

Neutron star history

- 1933: Baade and Zwicky proposed that supernova represents transition to NS

  $E_{SN} = 10^{53}$ erg = 0.1 M_{sun} c^2 = G $(M_{sun})^2/(10\ km)$

- Single neutron stars were too faint to be detected, unless they rotate and have magnetic field, to power pulsars
- 1964: discovery of bright radio source in Crab nebula (Hewish & Okoye)
- 1967: discovery of pulsars (Hewish & Bell-Burnell)

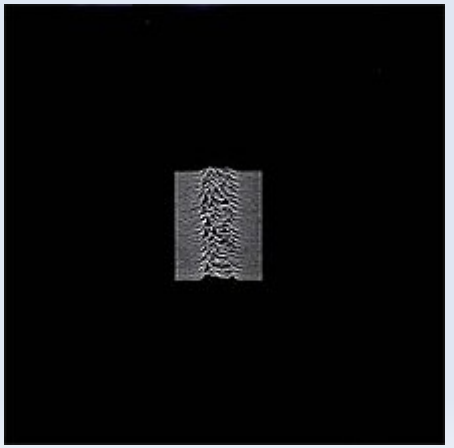

Neutron stars history

- 1967: Scorpuis X-1 establishes the first known accreting neutron star, whose X-ray emission comes from accretion disk
- Isolated neutron star in Optical band was identified by Hubble Telescope in 1997

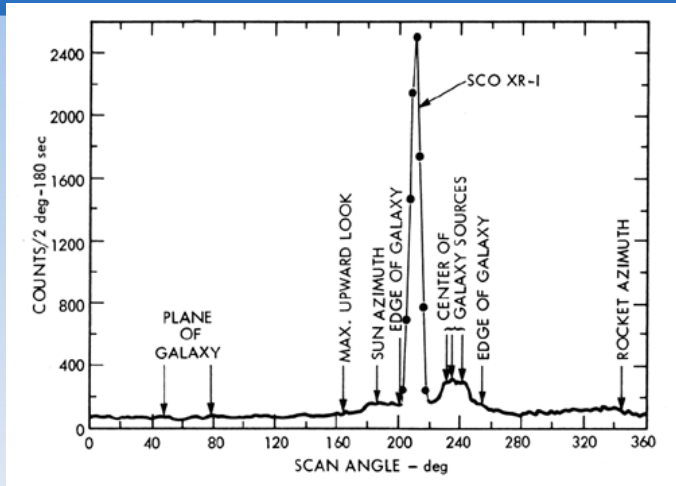

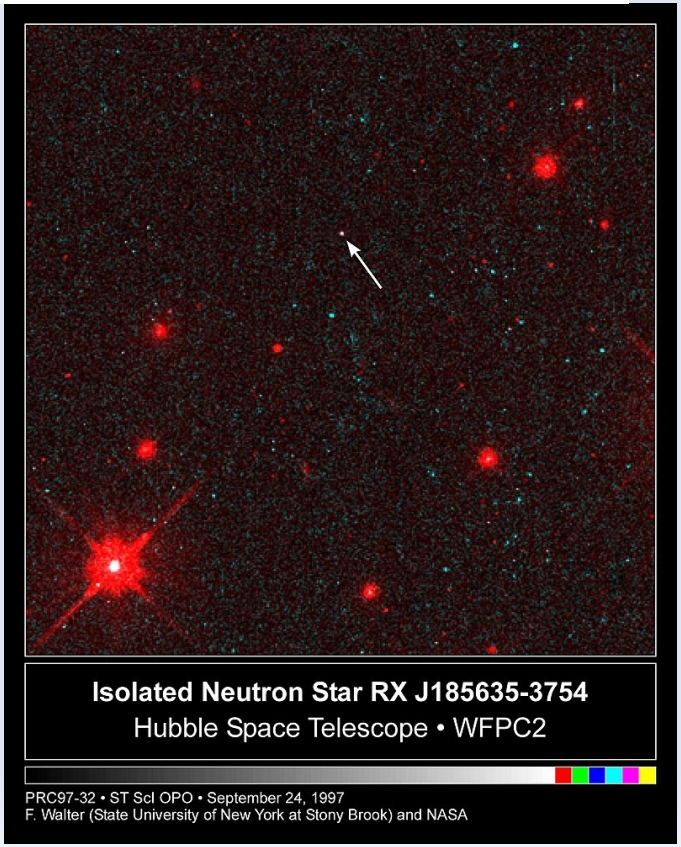

Neutron star matter

- Many-body system of strongly interacting particles (protons, neutrons, electrons, positrons, muons,…)
- The Equation of State (EoS) describes the composition and properties of these particles
- The matter inside the star is cold (T~0) but highly dense and degenerate. Pressure as a function of density is needed.
- EoS is affecting the mass-radius relation

Mass limit

- TOV = Tolman-Oppenheimer-Volkoff mass limit
- Results from GR hydrostatic equilibrium condition for a spherical object

$$\frac{dP}{dr} = \frac{-G\left(M(r) + 4\pi r^3 P/c^2\right)\left(\rho + P/c^2\right)}{r\left(r - 2GM(r)/c^2\right)}$$

$$\frac{dM(r)}{dr} = 4\pi\rho r^2$$

- For neutron star composed of completely degenerate Fermi gas, the limit is about 0.7 M_{sun} - less than Chandrasekhar limit for electrons

Mass limits

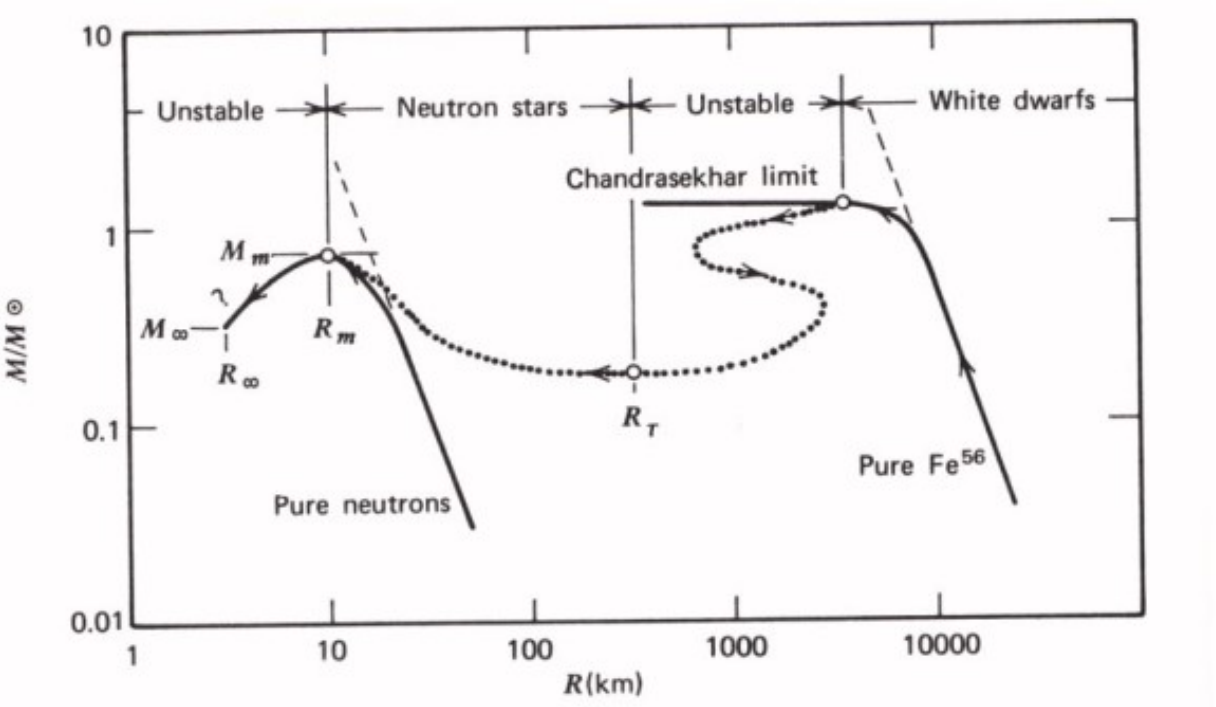

Figure 1: From Weinberg: Configurations of stellar equilibrium. The solid curves on the left and right represent the TOV solution for a pure neutron star and the Chandrasekhar solution for a pure ^{56}Fe white dwarf star, respectively. The dashed lines give the extrapolated nonrelativistic solutions in these two cases. The dotted line represents the interpolating solution of Harrison, Thorne, Wakano, and Wheeler, which takes into account the shift in chemical composition from ^{56}Fe to neutrons. Arrows indicate the direction of increasing central density. The various transitions between stability and instability occur at the maxima and minima of M, marked here with small circles.

Solutions for polytrope

For realistic P(ρ) relation, the TOV equation must be solved numerically, to obtain Mass-Radius relation. Alternatively, Lane-Emden equation may be solved (Newtonian limit)

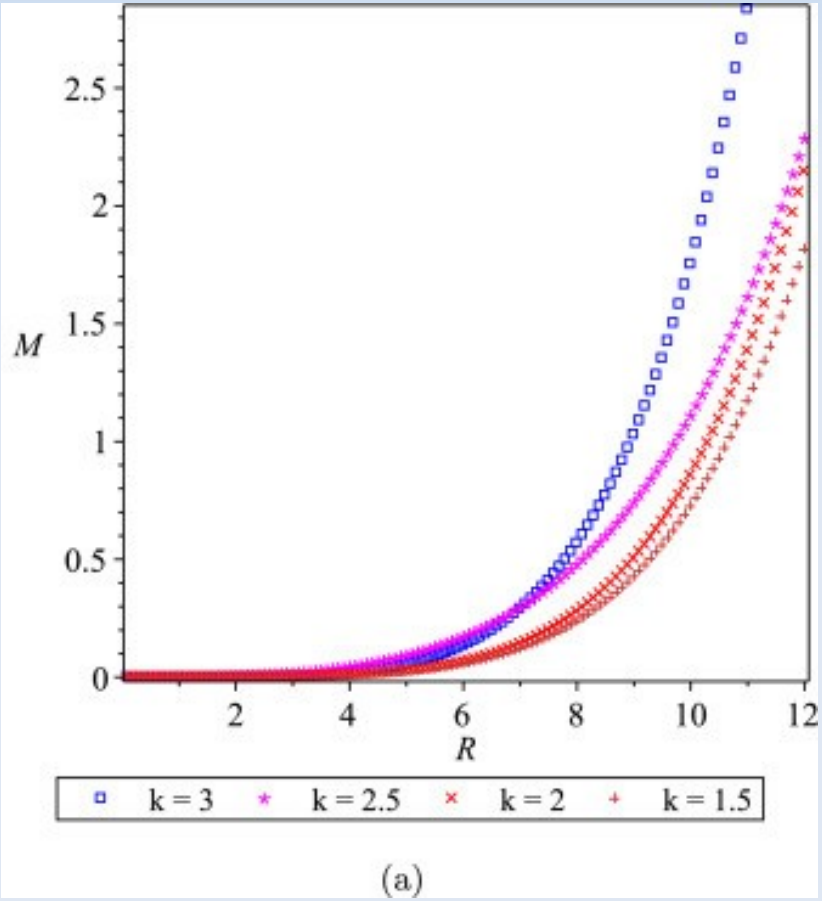

Variation of total mass with star radius with central density 0.7×10^{15} g/cm^3 for polytropes with k=3, 2.5, 2 and 1.5.

$$p = \rho^{1+1/k}$$

Neutron Star structure

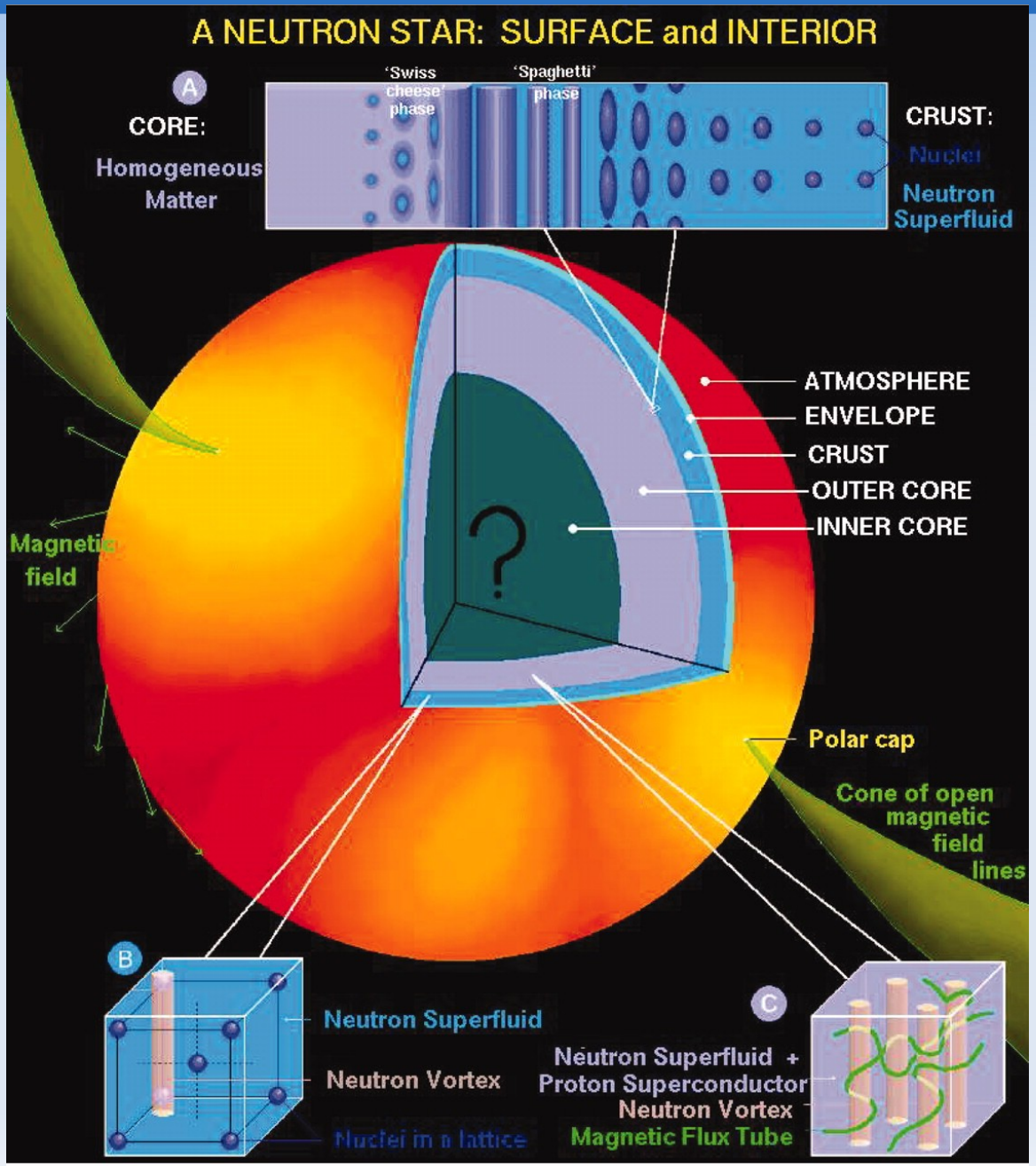

Lattimer & Prakash, 2004

EOS above neutron drip density

- With increasing density, nuclei become progressively more neutron rich due to electron captures, until neutrons start to drip out from nuclei at some treshold density, ρ_{drip}.
- Condition for drip: M(A,Z) = M(A-1, Z) + m_n and depends on detailed form of M(A,Z). Electron number density must provide their Fermi energy higher than loss of binding energy of the nucleus.
- The drip density is about $\rho_{drip} = 4 \times 10^{11}$ g/cm^3.
- Above the drip, volume of each nucleus becomes smaller, due to increased pressure. Electron Fermi level rises, and muons appear when $\rho = 3 \times 10^{14}$ g/cm^3

Nuclear ”pasta”

- Within the crust, above the neutron drip density of 4×10^{11} g/cm^3, neutron chemical potential is zero and neutrons leak out of nuclei.
- Continuous change of dimensionality of matter:
  - 3D nuclei (meatballs)
  - 2D cylindrical nuclei (spaghetti)
  - 1D slabs of nuclei, interlaid with planar voids (Lasagna)
  - 2D cylindrical voids (ziti)
  - 3D voids (ravioli)
  - Uniform matter (sauce)

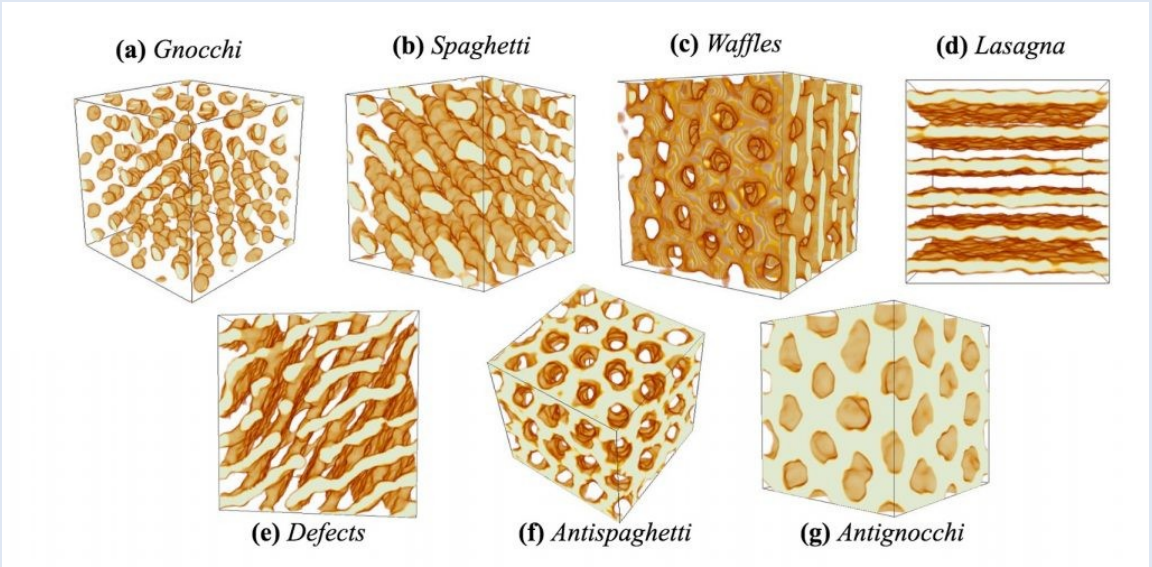

Core EOS

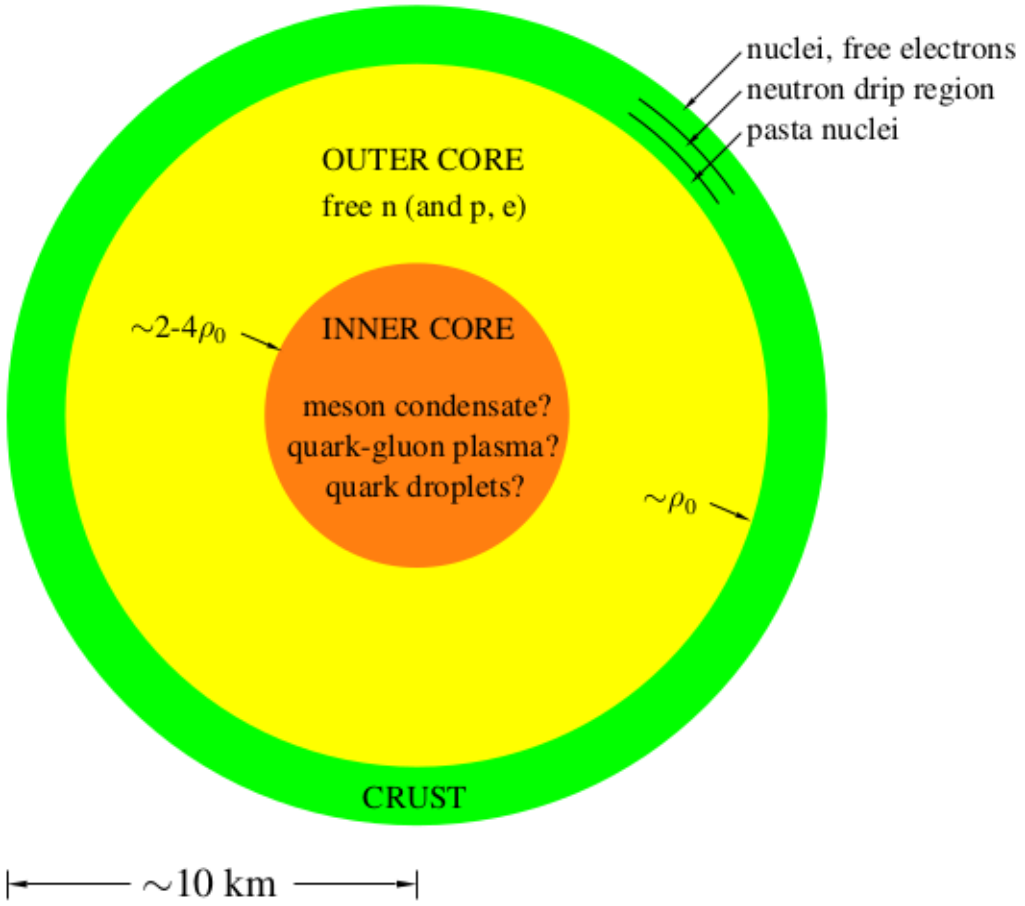

Figure 2: An illustration indicating the richness of the neutron star problem: the iron and free-electron surface; neutron drip as the nuclei are pressed closer together; interesting topological mixed phases that form as the matter makes the transition from nuclei to a nucleon gas; the free neutron (with some protons and electrons) outer core from 1-2 times nuclear density; a possible mixed phase (not shown) as the nucleon gas transitions to a more exotic dense phase; and the very dense inner core where exotic states of nuclear matter – pion or kaon condensates, free quarks or quark droplets, color-flavor-locked phases of nuclear matter – might exist.

Core EOS

- In the inner crust and outer core, the star composed of n-p-e-μ. EOS is found by many body calculations in quantum-mechanical or quantum-field theory.
- Unresolved issues of the core are about the way the quarks are grouped and whether strange quarks appear.
- Kaons are heavy version of pion (with s quark) and hyperons Lambda are a heavy version of neutron.

Alternative core compositions

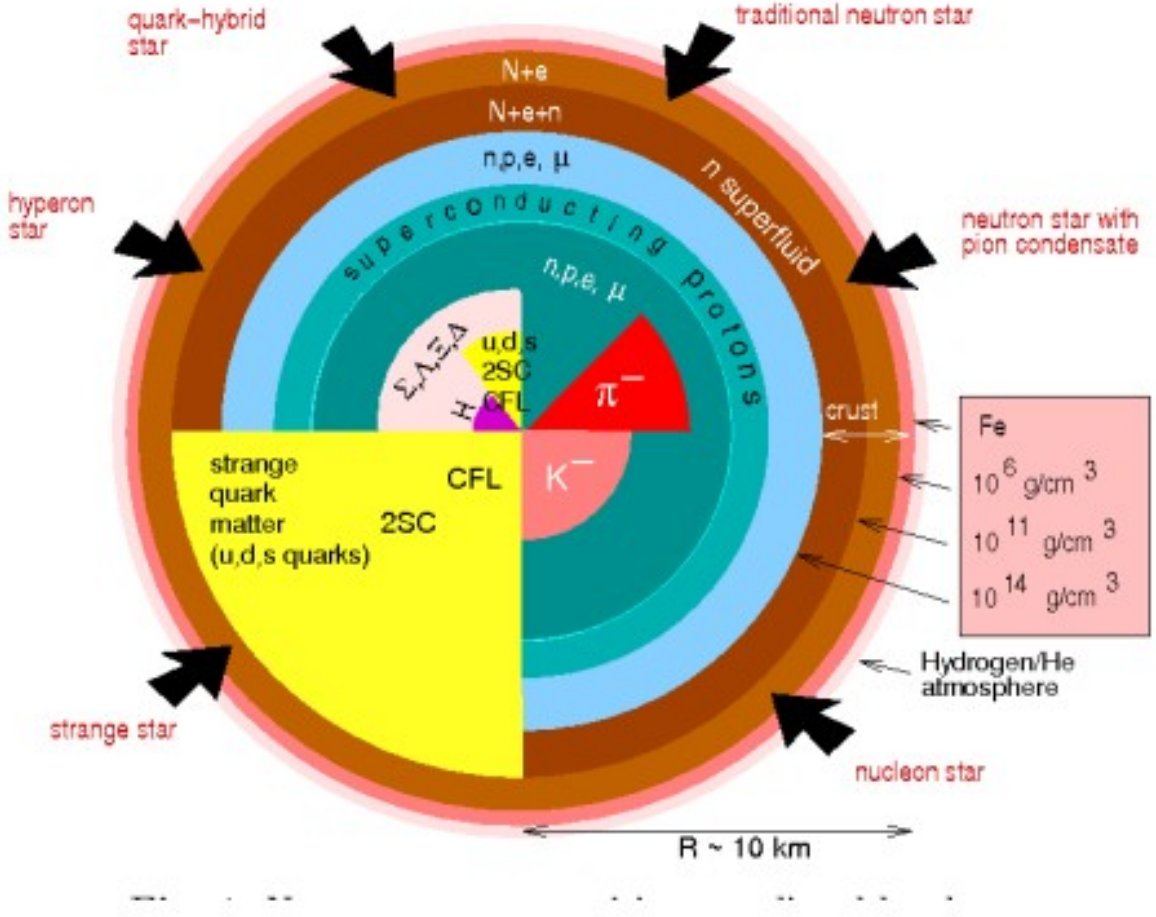

Figure 12: Alternate core compositions

Predictions of different EoS

- Nuclear equlibrium density found at laboratory nuclei is $n_0 = 0.16$ fm^{-3} for neutrons and protons.
- In neutron star core, density may be as high as 5-10 n_0. In addition, only few per cent of protons are contributed by high excess of neutrons.
- In the core, condensed mesons (kaon and pion), strangeness-bearing barions, and even deconfined quarks may appear.
- Different models predict up to factor 6 difference in pressure at density n_0

Predictions of Various EOS's

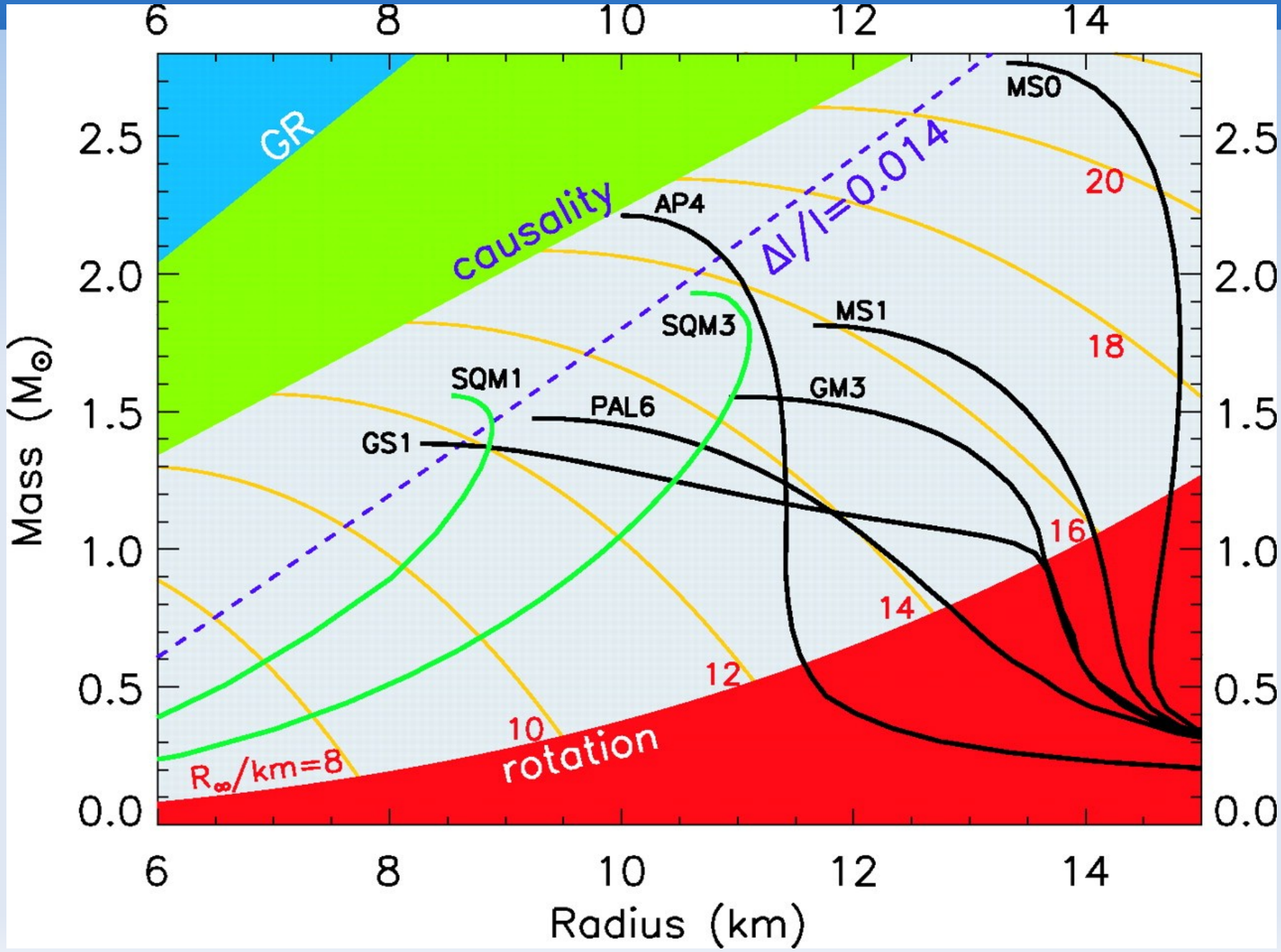

Summary of Equations of state

TABLE 1

EQUATIONS OF STATE

Symbol	Reference	Approach	Composition
FP	Friedman & Pandharipande (1981)	Variational	*np*
PS	Pandharipande & Smith (1975)	Potential	$n\pi^0$
WFF(1–3).....	Wiringa, Fiks & Fabrocine (1988)	Variational	*np*
AP(1–4)	Akmal & Pandharipande (1997)	Variational	*np*
MS(1–3)	Müller & Serot (1996)	Field theoretical	*np*
MPA(1–2).....	Müther, Prakash, & Ainsworth (1987)	Dirac-Brueckner HF	*np*
ENG	Engvik et al. (1996)	Dirac-Brueckner HF	*np*
PAL(1–6)	Prakash et al. (1988)	Schematic potential	*np*
GM(1–3)	Glendenning & Moszkowski (1991)	Field theoretical	*npH*
GS(1–2)	Glendenning & Schaffner-Bielich (1999)	Field theoretical	*npK*
PCL(1–2)	Prakash, Cooke, & Lattimer (1995)	Field theoretical	*np*HQ
SQM(1–3).....	Prakash et al. (1995)	Quark matter	Q (*u*, *d*, *s*)

NOTE.—"Approach" refers to the underlying theoretical technique. "Composition" refers to strongly interacting components (*n* = neutron, *p* = proton, H = hyperon, K = kaon, Q = quark); all models include leptonic contributions.

Observational determination of EoS

- For observed neutron stars, their masses and radii can be estimated. PSR 1913+16, $M=1.4408\ M_{sun}$ gives the lower bound for NS maximum mass.
- Some results for the M/R ratio exclude the most extreme equations of state
- Discovery of NS with mass of 2.08 Msun for PSR J0740+6620 (2019) rejected several EOS
- Still, the results are allowing for many different compositions and EoS is not fully constrained

Neutron star structure

- Envelope and atmosphere: shape emergent photon spectrum and release of thermal energy from the stars's surface
- Crust: composed of nuclei, from ^{56}Fe to A~200 with Y_p=0.1-0.2. Crust is a non-uniform lattice of neutron-rich atomic nuclei.
- Outer core: soup of nucleons, electrons and muons
- Inner core: exotic particles, hyperons, kaon/pion condensates. Core is a homogeneous mixture of particles

The EoS for the core and crust may be different, and is to be "glued", or a unified EoS is used.

Piecewise polytrope is working approximation.

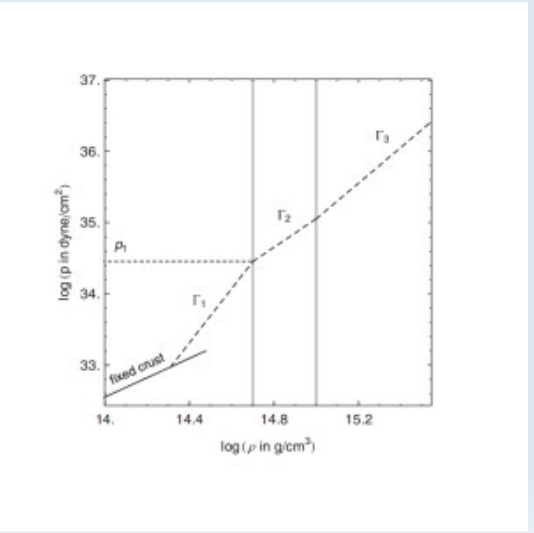

PSR J0952–0607

- PSR J0952–0607 has a mass of 2.35±0.17 M_{Sun}, making it the most massive neutron star known as of 2022.
- The pulsar likely acquired most of its mass by accreting up to 1 M_{Sun} of lost material from its companion
- It is called ”black widow”

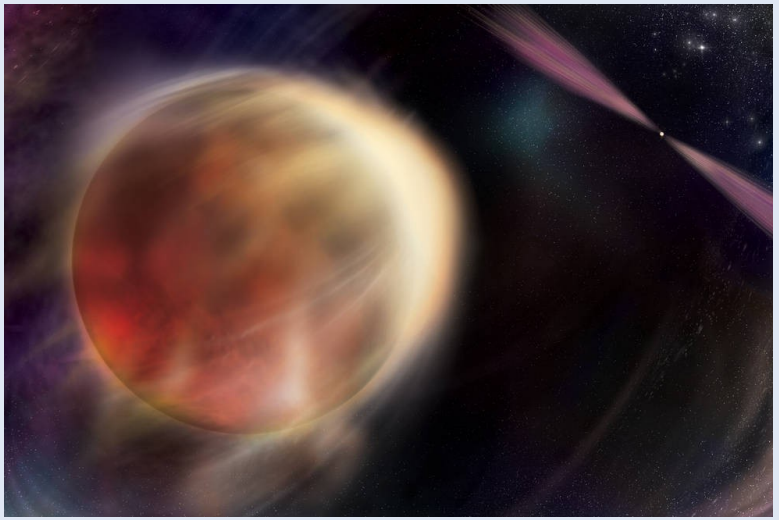

Break

Mass determination

- Most accurate determination from observations of binary pulsars.
- Orbital size and period from Doppler shifts → total mass of binary
- Shapiro delay: time delay is caused by spacetime dilation, which increases the path length for radio pulse
- Orbit shrinkage due to gravitational radiation allows for determination of each mass separately
- Mass can be also determined in X-ray binaries, but with large errors, and model-dependent (QPOs)

Observed double NS systems

TABLE I. Observational data of neutron stars in binary neutron-star systems containing a pulsar. Reported in the various columns are: the name of the binary, the total (gravitational) mass $M_{\rm tot}$, the (gravitational) masses of the pulsar and that of its neutron-star companion $M_{\rm A}, M_{\rm B}$, the mass ratio $q \leq 1$, the orbital period $T_{\rm orb}$, the projected semi-major axis of the orbit R (i.e., the projection of the semi-major axis onto the line of sight), the orbital eccentricity $e_{\rm orb}$, the distance from the Earth, the barycentric rotation frequency $f_{\rm s}$, and the inferred surface magnetic dipole field $B_{\rm surf}$. The data are taken from the respective references and truncated to four significant digits for the masses and to two significant digits for the rest. Note that in the case of the "double pulsar" system J0737-3039 (the only double system where both neutron stars are detectable as pulsars), the magnetic field of the second-formed pulsar (not reported in this table) is estimated to be 1.59E+12 G.

Name	$M_{\rm tot}$ $[M_\odot]$	$M_{\rm A}$ $[M_\odot]$	$M_{\rm B}$ $[M_\odot]$	q	$T_{\rm orb}$ [days]	R [light s]	$e_{\rm orb}$	D [kpc]	$f_{\rm s}$ [Hz]	$B_{\rm surf}$ [G]
J0453+1559 [8]	2.734	1.559	1.174	0.75	4.1	14	0.11	1.8	22	9.3E+09
J0737-3039 [9]	2.587	1.338	1.249	0.93	0.10	1.4	0.088	1.1	44	6.4E+09
J1518+4904 [10]	2.718	<1.766	>0.951	>0.54	8.6	20	0.25	0.7	24	9.6E+08
B1534+12 [11]	2.678	1.333	1.345	0.99	0.42	3.7	0.27	1.0	26	9.6E+09
J1753-2240 [12]	–	–	–	–	14	18	0.30	3.5	10	9.7E+09
J1756-2251 [13]	2.577	1.341	1.23	0.92	0.32	2.8	0.18	0.73	35	5.4E+09
J1807-2500B [14]	2.571	1.366	1.21	0.89	1.0	29	0.75	–	239	≤9.8E+08
J1811-1736 [15]	2.571	<1.478	>1.002	>0.68	19	35	0.83	5.9	9.6	9.8E+09
J1829+2456 [16]	2.59	<1.298	>1.273	>0.98	1.2	7.2	0.14	0.74	24	1.5E+09
J1906+0746 [17]	2.613	1.291	1.322	0.98	0.17	1.4	0.085	7.4	6.9	1.7E+12
J1913+1102 [18]	2.875	<1.84	>1.04	>0.56	0.21	1.8	0.090	13	1.1	2.1E+09
B1913+16 [19]	2.828	1.449	1.389	0.96	0.32	2.3	0.62	7.1	17	2.3E+10
J1930-1852 [20]	2.59	<1.199	>1.363	>0.88	45	87	0.40	2.3	5.4	6.0E+10
B2127+11C [21]	2.713	1.358	1.354	1.0	0.34	2.5	0.68	13	33	1.2E+10

Baiotti & Rezzola 2017

Neutron stars in X-ray binaries

Table 3 Masses of Neutron Stars in High-Mass and Low-Mass X-ray Binaries

System	M_{NS} ($M_\odot$)	Error ($M_\odot$)	References
Neutron Stars in High-Mass X-ray Binaries			
LMC X- 4	1.57	0.11	1
Cen X- 3	1.57	0.16	1
4U 1538- 522	1.02	0.17	1
SMC X- 1	1.21	0.12	1
SAX J1802.7- 2017	1.57	0.25	1
XTE J1855- 026	1.41	0.24	1
Vela X- 1	2.12	0.16	1
EXO 1722- 363	1.91	0.45	1
OAO 1657- 415	1.74	0.30	1
Her X- 1	1.07	0.36	1
Neutron Stars in Low-Mass X-ray Binaries			
4U 1608- 52	1.57	$^{+0.30}_{-0.29}$	2
4U 1724- 207	1.81	$^{+0.25}_{-0.37}$	2
KS 1731- 260	1.61	$^{+0.35}_{-0.37}$	2
EXO 1745- 248	1.65	$^{+0.21}_{-0.31}$	2
SAX J1748.9- 2021	1.81	$^{+0.25}_{-0.37}$	2
4U 1820- 30	1.77	$^{+0.25}_{-0.28}$	2
Cyg X- 2	1.90	$^{+0.22}_{-0.35}$	3

Notes. 1. See Falanga et al. (2015), Özel et al. (2012), Rawls et al. (2011), and references therein. We exclude 4U 1700- 377, for which there is no evidence that it is a neutron star. 2. See Özel et al. (2015) for the latest constraints. 3. Orosz & Kuulkers (1999).

NS masses from pulsar timing

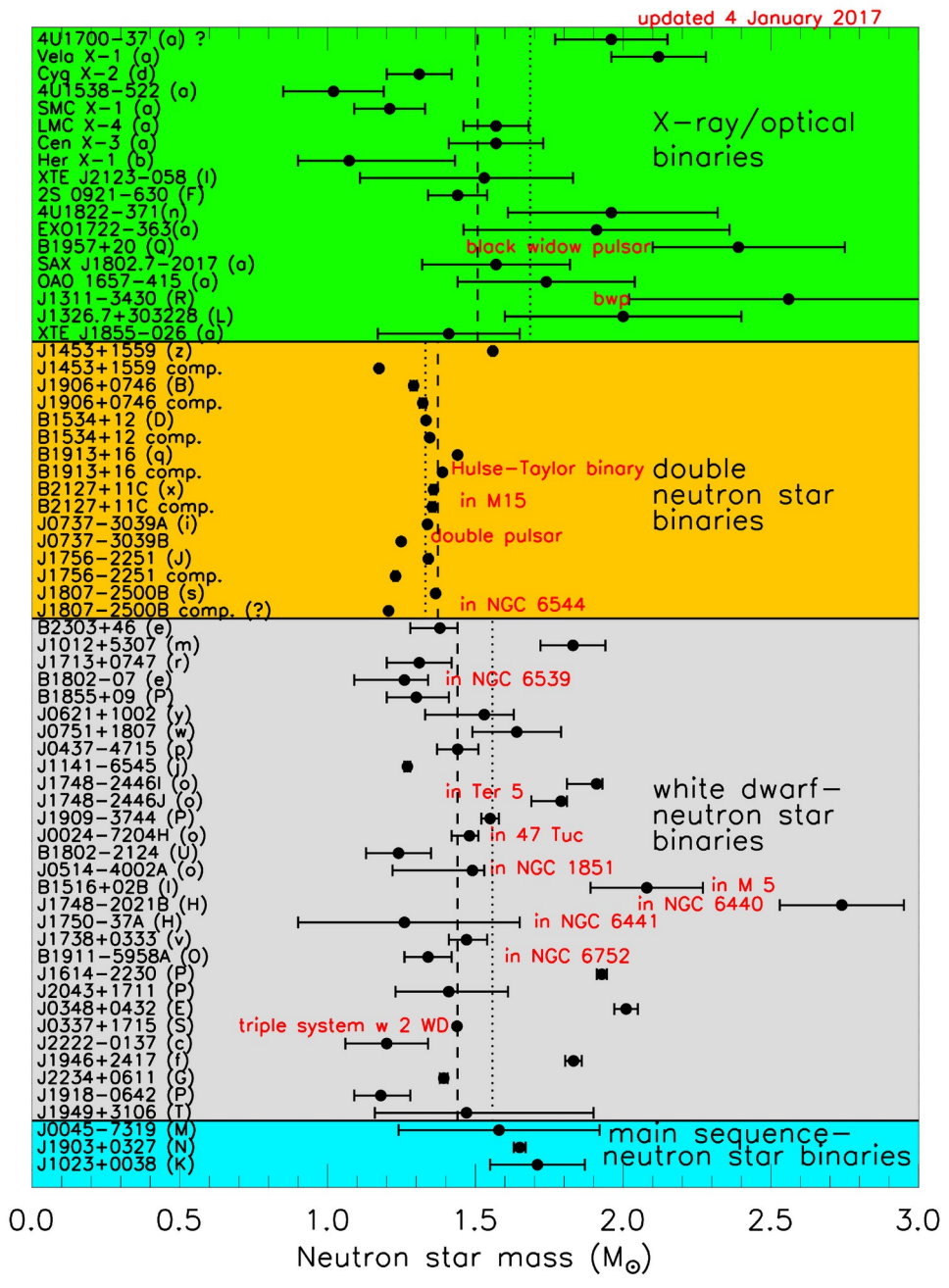

Masses measured from pulsar timing. Vertical dashed (dotted) lines indicate category error-weighted (unweighted) averages. The figure is updated from that of Lattimer (2014)

Rotation of the star

- Neutron stars have both minimum and maximum mass.
- Causality: speed of sound must be less than speed of light. Constraints the maximum mass.
- Upper limit for NS spin frequency is the mass-shedding, when the rotation is Keplerian

$$\nu_K = \frac{1}{2}\pi\sqrt{\frac{GM}{R^3}} = 1833\left(M/M_{Sun}\right)^{1/2}\left(10\,km/R\right)^{3/2}\,Hz$$

- Highest known rotation period 641 Hz of PSR B1937+21 implies radius limit of 15.5 km for M=1.4

NS-NS mergers

- Binary NS may form after the common evolution of binary stars
- Alternatively, the second NS may be captured in dense stellar system
- Merger will lead to observable electromagnetic signal (GRB)
- Signal delayed, if the product is first a hypermassive neutron star

Simulations

An example of the dynamics of an unequal-mass binary with an ideal-fluid EOS.

Figure shows isodensity contours in the equatorial plane for the inspiral and merger of a binary with a mass ratio

$q = M_{B/}M_A = 0.7$

and a total gravitational mass

$M_{tot} = M_B + M_A = 3.07 M_{sun}$.

During the inspiral phase, the heavier and more compact star is only slightly affected by its companion, whereas the latter is decompressed rapidly while being accreted onto the heavier star

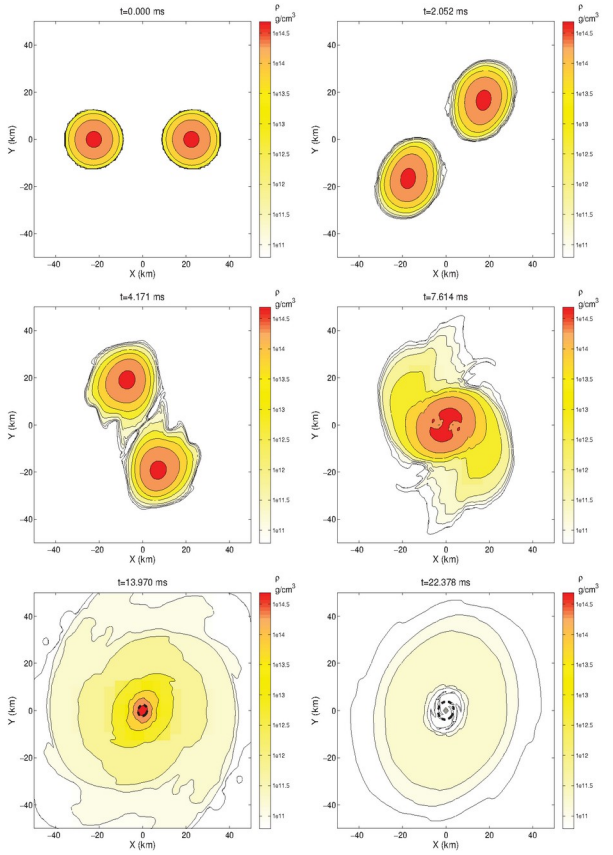

FIG. 3. Isodensity contours in the (x, y) plane for the evolution of a high-mass (individual stellar rest mass $1.625 M_\odot$) binary with an ideal-fluid EOS. The thick dashed lines in the lower panels show the location of the apparent horizon. [Reprinted with permission from Ref. [32]. © (2008) by the American Physical Society.]

Simulations

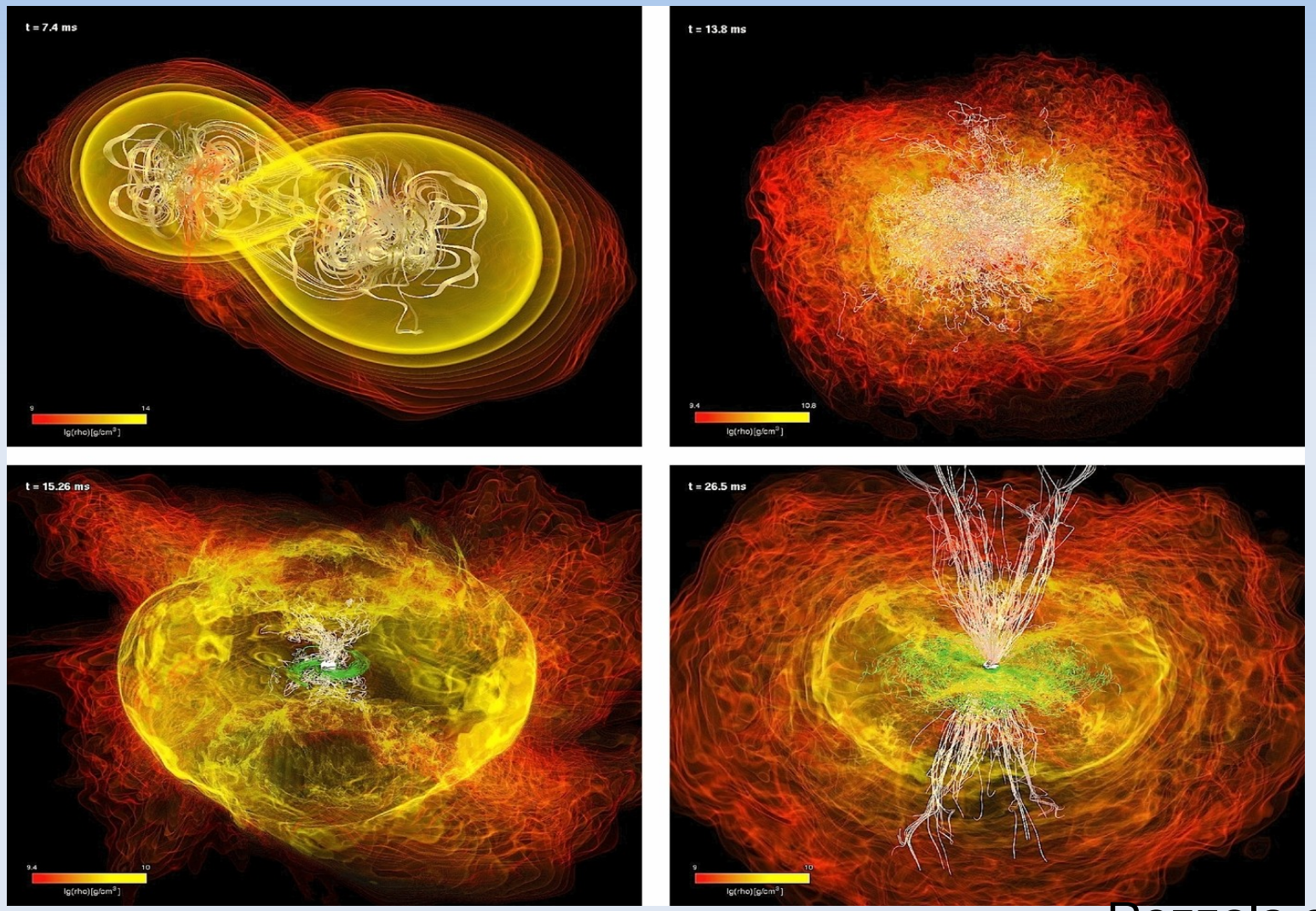

Rezzola et al. 2014

Snapshots at representative times of the evolution of the binary and of the formation of a large-scale ordered magnetic field. Shown with a color-code map is the density, over which the magnetic-field lines are superposed. The panels in the upper row refer to the binary during the merger (t = 7.4 ms) and before the collapse to BH (t = 13.8 ms), while those in the lower row to the evolution after the formation of the BH (t = 15.26 ms, t = 26.5 ms). Green lines sample the magnetic field in the torus and on the equatorial plane, while white lines show the magnetic field outside the torus and near the BH spin axis. The inner/outer part of the torus has a size of ~90/170 km, while the horizon has a diameter of 9 km.

Are jets produced?

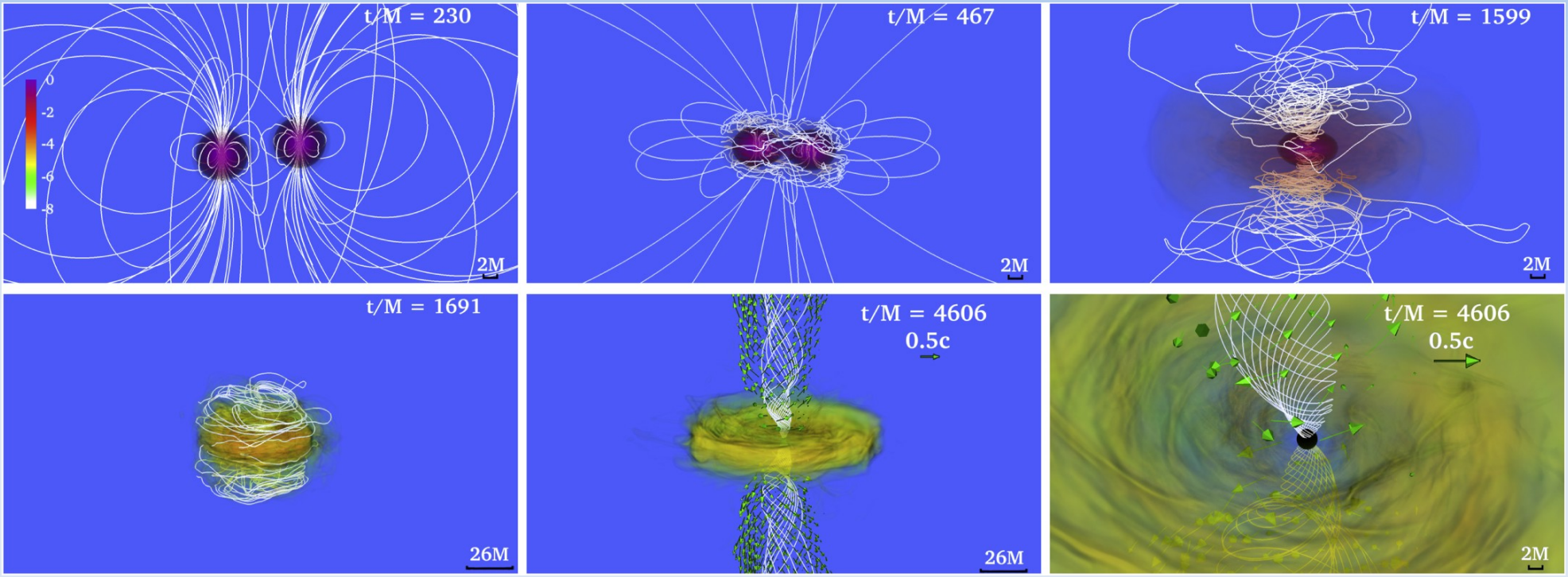

Ruiz et al. 2016

Snapshots of the rest-mass density, normalized to its initial maximum value ρ0,max = 5.9e14 (log scale) at selected times. The arrows indicate plasma velocities, and the white lines show the B-field structure. The bottom middle and right panels highlight the system after an incipient jet is launched. Neutron star mass Mns=1.625 Msun.

Jet in GW 170817

- Gravitational wave signal from the merger of a binary neutron-star (NS-NS) system was achieved (GW170817)
- It was also accompanied by an electromagnetic counterpart -- the short-duration GRB 170817A.
- It occurred in the nearby (D≈40Mpc) elliptical galaxy NGC4993, and showed optical, IR and UV emission from half a day up to weeks after the event, as well as late time X-ray (at ≥8.9days) and radio (at ≥16.4days) emission.
- There was a delay of $\Delta t \approx 1.74$s between the GW merger chirp signal and the prompt-GRB emission onset, and an upper limit of $\theta_{obs} < 28^\circ$ was set on the viewing angle w.r.t the jet's symmetry axis from the GW signal (Granot et al. 2017)

Neutron star merger

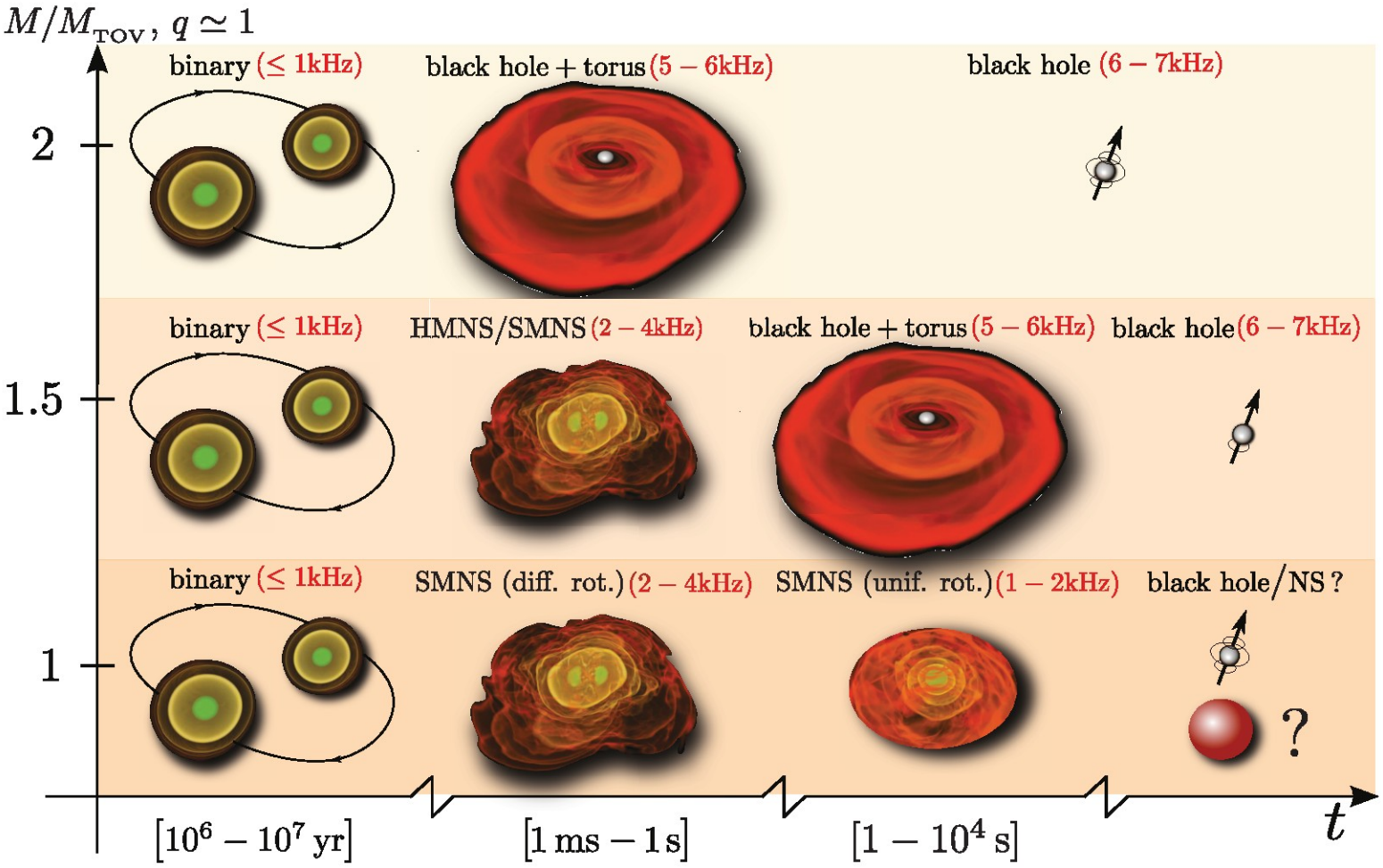

Baiotti & Rezzola 2017

Hypermassive neutron star

- A hypermassive neutron star (HMNS) is a neutron star with sufficient mass to collapse into a black hole, and is more massive than the Tolman-Oppenheimer-Volkoff limit.
- It immediately collapses unless rotation counteracts the effect of gravity and delays the collapse.
- The term supramassive neutron star (SMNS) has a similar meaning: sometimes intended to mean "longer-lived than a HMNS" and sometimes assuming HMNS to be a sub-type.

HMNS in GW 170817 merger

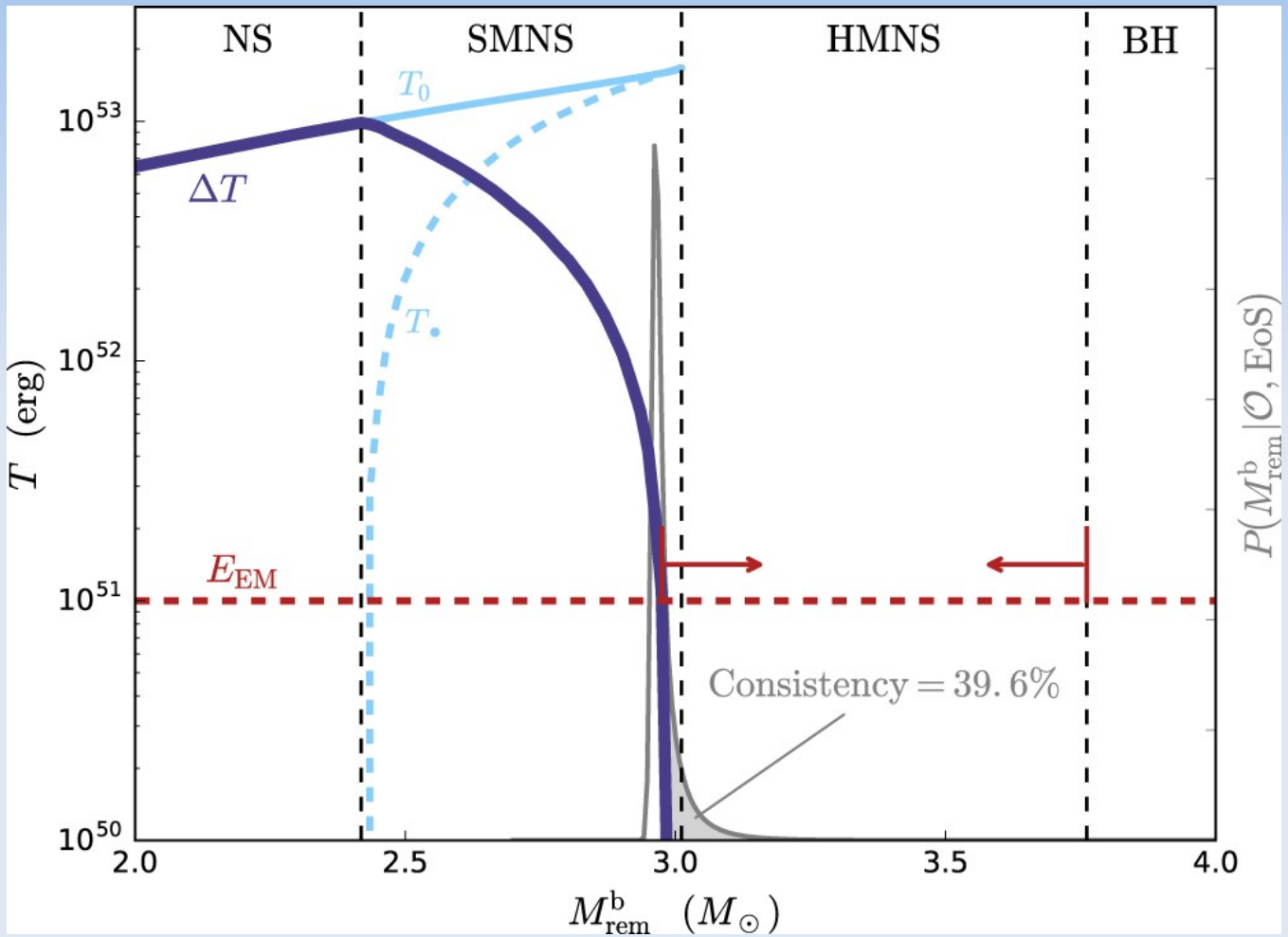

Maximum extractable rotational energy of the merger remnant ΔT=T0−T, shown as a dark-blue solid curve for a sample EOS. Vertical dashed curves demarcate the range of baryonic remnant masses for which the immediate post-merger compact object is a stable NS, SMNS, HMNS, or a BH (prompt collapse). A horizontal red dashed curve shows the maximal energy transferred to the environment of the merger consistent with EM observations of GW170817 for the GRB and KN emission. The parameter space where ΔT⩾EEM is thus ruled out. The prompt-collapse scenario is also ruled out, such that Mass of remnant is constrained within an “allowed” region shown by red arrows. The gray curve shows the remnant mass probability distribution function. (**Margalit & Metzger 2017)**

Constraints on M-R from GW170817

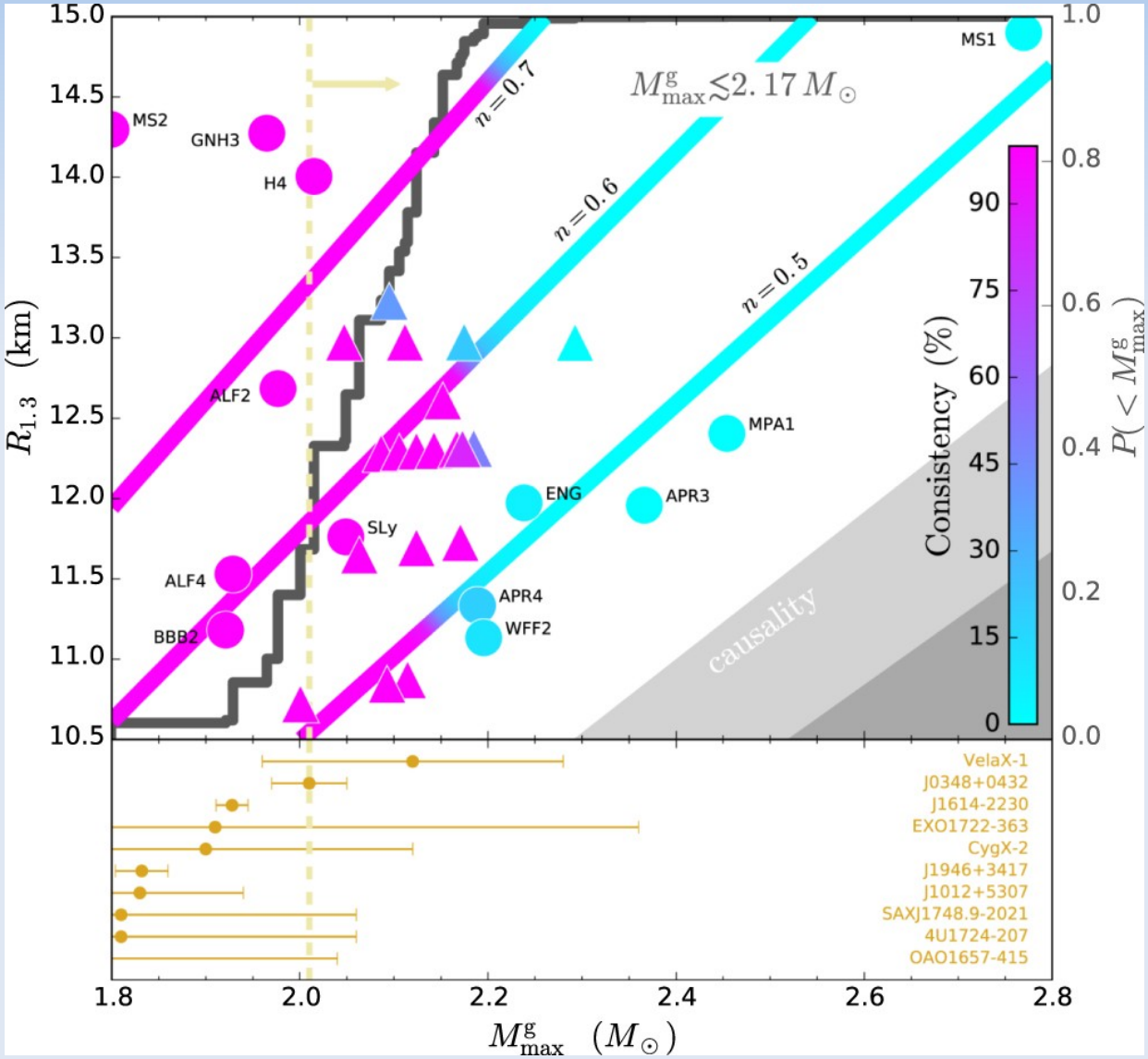

Constraints on properties of the NS EOS—radius of a 1.3M⊙ NS, R1.3, and maximal non-rotating gravitational mass, Mgmax—based on joint GW-EM observations of GW170817. Different EOSs are represented as points, the color of which corresponds to the consistency of the given EOS with observational constraints. The similarly colored diagonal curves represent polytropic EOSs of index n, while the gray shaded regions to the bottom right are ruled out by the requirement of causality.

Clearly, a low NS maximal mass is preferred due to constraints ruling out SMNS formation. The background gray curve shows the cumulative probability distribution function that the maximum mass Mgmax is less than a given value, from which we find Mgmax□2.17M⊙ at 90% confidence.

The bottom panel shows masses of observed Galactic NSs, from which a lower limit on Mgmax can be placed (vertical dashed line).

Dynamics of post-BNS merger

- Mass is ejected from the system as a result of: dynamics (shock heating), or secular process (magnetically or neutrino-driven winds)
- More ejected mass results in higher rate of synthesis of elements (Kilonova emission)
- Eccentric mergers may occur in dense stellar systems (globular clusters) and thus amount of ejected matter is maximized

Next week

- Pulsars

Further reading:

- Ozel & Freire, ”Masses, Radii & EOS of neutron stars”, ARAA, 2016, arXiV:1603.02698
- M. Oertel et al., ”Equations of state for supernovae and compact stars” arXiV:1610.03361
- L. Baiotti and L. Rezzola, ”Binary neutron-star mergers: a review of Einstein's richest laboratory”, arXiV:1607.03540